Journal of Materials Chemistry C

RSC Publishing

PAPER

View Article Online
View Journal | View Issue

Cite this: *J. Mater. Chem. C*, 2013, **1**, 6386

Structurally simple thienodipyrandione-containing reversible fluorescent switching piezo- and acidochromic materials†

Rajeswara Rao M, Chia-Wei Liao and Shih-Sheng Sun*

Received 1st August 2013
Accepted 5th August 2013

DOI: 10.1039/c3tc31504e

www.rsc.org/MaterialsC

We report here the structure–property correlations of a series of anthracene/pyrene derivatives grafted on a rigid, planar, and well conjugated endo-cyclic alkenyl lactone (thienodipyrandione) that exhibited aggregation induced emission. Unlike typical vinylene based solid-state fluorescence materials, rigid thienodipyrandione moieties can bestow a higher order of conformational twist as well as enhanced intermolecular interactions by C–H···O interactions due to the presence of a carbonyl group that leads to enhanced thermal stability. Compounds **TDAn** and **TDAnPh** exhibit distinct piezofluorochromic properties in which emission colors can be switched by grinding and heating. Based on a variety of spectroscopic techniques including XRD, DSC, and NMR, the observed piezochromic emission is attributed to the result of phase transition from structural crystalline (order) to amorphous (disorder) state or *vice versa*. Most uniquely, one of the anthracene derivatives, **TDAn**, displayed specific acidofluorochromism whereas the other congener, **TDAnPh**, did not, even though they are structurally very similar. Crystal structure analysis revealed that a combination of various secondary interactions such as C–H···O, π–π and C–H···π interactions all play key roles in the supramolecular assemblies to display such distinctive features. The current study has disclosed a class of new stimuli-responsive materials with great potential in applications for micro-environmental sensing, optical switching and recording.

Introduction

The fundamental and essential issue in materials chemistry is to understand the electronic interactions and self-assembly in molecular solids which play a crucial role in determining the ultimate optoelectronic properties. The design and synthesis of solid-state luminophoric materials have received tremendous attention in both scientific research and practical aspects owing to their potential applications in the field of optical and optoelectronic devices.[1] Especially, the correlations between the molecular stacking mode and modulated optical properties in order to improve and refine the design concept to develop materials with desired properties. The ability to manipulate the photoluminescence (PL) of organic materials is an important aspect due to the diverse applications such as sensors,[2] security inks,[3] re-healable materials,[4] shape memory materials,[5] and light-emitting diodes.[6] A great deal of synthetic effort has been devoted to develop these materials to achieve color tuning and excellent PL properties. One of the recent goals for practical applications is the control of the molecular packing mode instead of chemical alteration of the molecules.[7] Since luminescence properties of organic solids greatly depend on the molecular packing and intermolecular interactions, tunable solid-state emission could be realized through an external stimulus affecting the mode of molecular packing. In this regard, stimuli-responsive fluorescence switching, such as piezochromism,[8] vapochromism,[9] light,[10] thermo-[11] and acid-dependent[12] luminescence, of smart materials has received unprecedented attention.

The first fluorescence color switching compound based on a pressure stimulus with aggregation induced emission (AIE) property was reported by Park in 2010[8a] and followed by a number of new fluorescence color switching compounds synthesized by many others.[8b–m] Nevertheless, few examples of stimuli-responsive fluorescent materials with AIE properties have been successfully developed to date.[8–12] These materials are currently still in the initial stage of investigation and an in-depth understanding of the structure–property relationships of solid-state emission behavior is mandatory in order for better design and development of materials with intriguing properties. In particular, multi-stimuli responsive materials are extremely rare.[12a,13] Thus, there is a great demand to exploit new stimuli-responsive materials such as piezochromic fluorescent

Institute of Chemistry, Academia Sinica, 115 Nankang, Taipei, Taiwan, Republic of China. E-mail: sssun@chem.sinica.edu.tw; Fax: +011-886-2-27831237; Tel: +011-886-2-27898596

† Electronic supplementary information (ESI) available: Characterization data, UV-vis, fluorescence spectra, and photographs. CCDC 919160 and 919162. For ESI and crystallographic data in CIF or other electronic format see DOI: 10.1039/c3tc31504e

(PCF) materials and the investigation of their properties is highly desirable.

Within this line of idea, various 9,10-distyrylanthracene derivatives have been investigated as piezochromic fluorescent materials.[14] Interestingly, in most of the anthracene based PCF materials, a common structural design is merely to change the substituents at the styryl positions. In the pursuit to gain deeper insights and to establish in-depth structure–property correlations as well as for more potential practice applications, it is highly desirable and indeed indisputable to extend the scope of advanced material designs exhibiting PCF behavior. By keeping these in mind, through a judicious structural design, we have prepared a new building block, thienodipyrandione (TDP), which is a rigid, planar, and well-conjugated endo-cyclic alkenyl lactone. The TDP moiety has been introduced between two anthracene or pyrene groups to explore the PCF properties. We envisaged that a rigid TDP moiety would bestow a higher order of conformational twist compared to simple vinylene moiety as well as to induce unique supramolecular stacking architectures associated with various secondary intermolecular interactions. In addition, these cooperative supramolecular interactions can further increase the thermal stability of the resulting PCF materials, which is also an issue of concern for practical applications.[14a]

We report herein the structure–property correlations of aggregation-induced emission (AIE) and PCF behavior of phenyl anthracene (**TDAnPh**), and pyrene (**TDPy**) molecules (Scheme 1). The photophysical properties and AIE property of these molecules induced by the intermolecular interactions were rationalized by their X-ray crystal structures and theoretical calculations (B3LYP/6-31G(d)). In particular, the **TDAn** and **TDAnPh** exhibited an interesting piezo-fluorochromism, and the color changes in solid-state emission could be repeated many times, indicative of an excellent reversibility in the switching processes. Moreover, **TDAn** exhibits a unique acidofluorochromism based on a combination of subtle intermolecular interactions.

Results and discussion

Synthesis

The three target compounds **TDAn**, **TDAnPh**, and **TDPy** were synthesized by palladium catalyzed cross-coupling of 2,5-dibromo-3,4-diethylcarboxylthiophene **4** with corresponding aromatic alkynes followed by acid catalyzed cyclization (Scheme 1). All compounds were purified by column chromatography and re-crystallization process and the purified materials were fully characterized by various spectroscopic techniques. Full synthetic details are given in the experimental section.

Optical properties

The absorption spectra of **TDAn** and **TDAnPh** in dilute toluene solution exhibited absorption bands at 391 and 398 nm, respectively, with characteristic anthracene vibrational features, while **TDPy** (420 nm) displayed a broad spectral profile (Fig. S23, S24, and S25 ESI†). The bathochromic shift in the absorption spectrum of **TDPy** to its anthracene congener suggests enhanced conjugation in the π framework of **TDPy**. Furthermore, all compounds in their dilute solutions, regardless of the solvents used, were weakly fluorescent with broad structureless emission profiles (Fig. 1). Interestingly, the Stokes shifts for all compounds were large, *i.e.* 8128 cm^{-1}, 8205 cm^{-1}, and 5222 cm^{-1} in toluene solutions for **TDAn**, **TDAnPh**, and **TDPy**, respectively, indicative of large geometrical changes between the ground- and excited-state conformations. A large Stokes shift typically indicates a change in geometry from the highly twisted ground state to the more planar excited state or *vice*

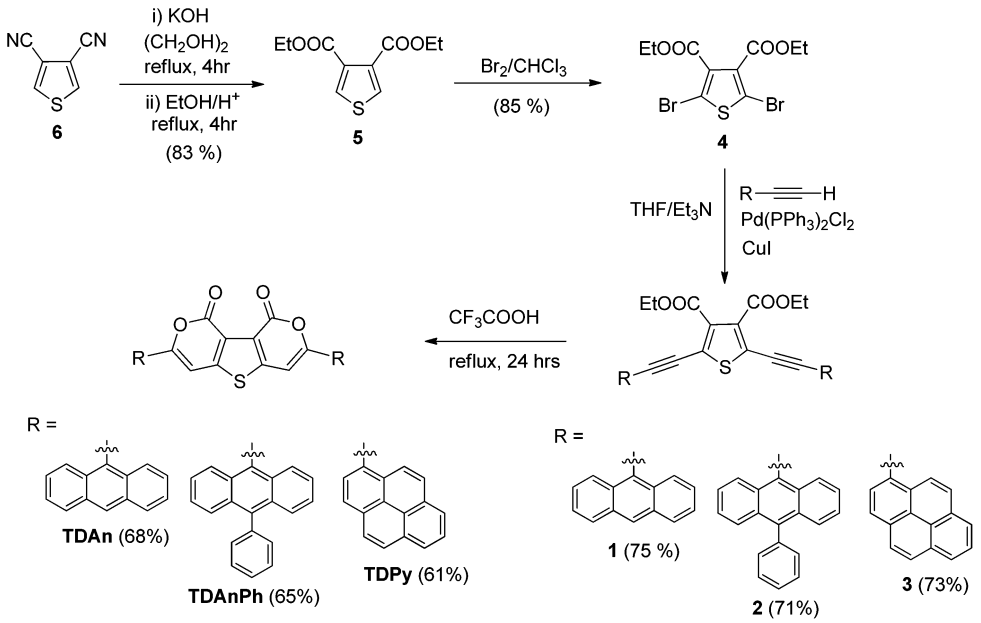

Scheme 1 Synthetic scheme of TDP based AIE molecules **TDAn**, **TDAnPh** and **TDPy**.

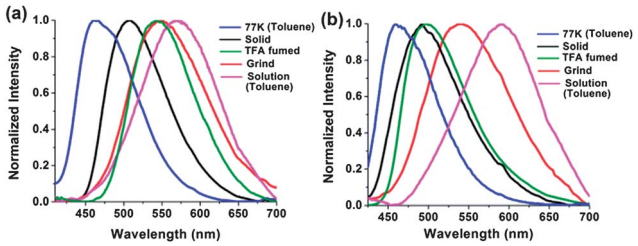

Fig. 1 The normalized PL spectra of **TDAn** (a) and **TDAnPh** (b) at various states and conditions.

versa.[15] It is worth mentioning that no concentration (1×10^{-4} to 1×10^{-7} M) dependent emission spectra were observed for any of the compounds, which precludes excimer formation.

TDP derivatives displayed a minor red shift in the solid-state absorption spectra compared to the absorption spectra in solution. In contrast, the emission maxima in the solid state are very different from those in solution. Relatively strong green and bluish green fluorescence were observed for **TDAn** and **TDAnPh** with maxima at 507 (Φ_f = 12.7%) and 491 nm (Φ_f = 21.6%), respectively, which are blue shifted 64 and 100 nm, respectively, with respect to the emissions in toluene solutions (Φ_f = 8.3% for **TDAn** and Φ_f = 6.2% for **TDAnPh**) (Fig. 1a and b). The significant blue shift of the solid-state emission implies a distorted and highly twisted arrangement in the solid state which limits effective conjugation and results in blue-shifted emission to that in solution. In the case of **TDAnPh**, further blue-shift can be ascribed to the increased structural twist by the additional phenyl substitution. The increased emission intensity could be attributed to the aggregation induced emission (AIE) enhancement. Surprisingly, unlike **TDAn** and **TDAnPh**, **TDPy** showed no solid-state emission (Fig. S26 ESI†).

TDP derivatives render no change in the glassy-state absorption spectra compared to the absorption spectra in solution indicating that compounds in both solution and glassy state possess similar rigid ground state conformations (Fig. S27 ESI†). In contrast, like in the solid-state, the emission maxima in glassy state are different from those in solution. Both **TDAn** and **TDAnPh** emitted intense blue fluorescence in toluene or 2-methyl THF glass at 77 K (Fig. 2) with an emission band centered at 463 nm, which was significantly blue-shifted from their room-temperature solution emission maxima at 571 and 591 nm for **TDAn** and **TDAnPh**, respectively. Moreover, **TDAnPh** exhibited a structured emission spectrum (Fig. S28 ESI†). On the other hand, **TDPy** showed very weak emission at 505 nm in 2-methyl THF–toluene glass at 77 K with a modest shift in the band position compared to its emission at 538 nm in solution (Fig. S29 ESI†). Noticeably, the Stokes shifts for **TDAn** (3370 cm^{-1}), **TDAnPh** (2917 cm^{-1}) and **TDPy** (3895 cm^{-1}) in a 2-methyl THF glass were significantly small compared to their solution state, strongly emphasizing that the structural relaxation in the excited state was prohibited. On the other hand, as anticipated, the fluorescence quantum yields in 2-methyl THF glass were quite high compared to their corresponding solutions and were 49%, 60% and 42% for **TDAn**, **TDAnPh** and **TDPy**, respectively. Similar to the emission properties in the solid state, the substantial blue shift of **TDAn** and **TDAnPh** in glassy state suggests a highly conformational twist in molecular structure compared to the one in solution. In the case of **TDPy**, the minor blue shift of the emission in the glassy state strongly intimates minor conformational change of the molecule.

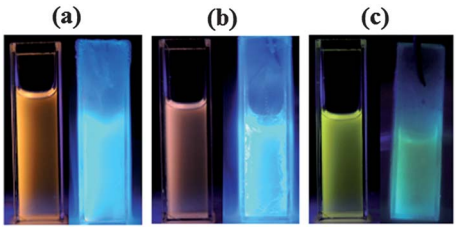

Fig. 2 Photographs of 2-methyl THF solutions (5×10^{-6} M) of **TDAn** (a), **TDAnPh** (b) and **TDPy** (c) at ambient temperature (left) and 77 K (right).

Geometry optimized structures

The optimized geometry structures by Gaussian 09 at B3LYP/6-31G(d) level revealed that all three TDP derivatives adopt a twisted spatial conformation. The dihedral angles of the TDP core and the peripheral aromatic moieties differed among each compound with 61.99°, 64.89° and 40.43°, respectively, for **TDAn**, **TDAnPh** and **TDPy** (Fig. 3). The relatively small torsional angle in the case of **TDPy** is attributed to the reduced internal steric hindrance. Even though the optimized structure of **TDPy** in the gas phase shows some structural distortion, the observations of minor blue shift in the emission of **TDPy** in glassy state at 77 K and no emission in solid state indicate that the quenching of emission in solid state is likely due to the prominent intermolecular interactions through the pyrene moieties. Relatively weak steric repulsive interactions between central TDP and the peripheral pyrene moieties might escalate the planarization of the molecule in the solid-state which in turn favors the intermolecular interactions. The observation of prominent red-shift in the absorption maxima of **TDPy** compared to its anthracene congeners supports the notion. To obtain further insights in the aggregation-induced emission of **TDAn**, **TDAnPh** and **TDPy**, we have attempted to grow single crystals. Single crystals of **TDAn** and **TDAnPh**, suitable for X-ray diffraction analysis, were successfully obtained by slow cooling of a hot DMSO solution of **TDAn** and slow evaporation of a $CHCl_3$ solution of **TDAnPh**, respectively. The molecular structures of **TDAn** and **TDAnPh** are presented in Fig. 3. Both crystals are monoclinic with space groups of *C*2/*c* and *C*2/*m* for **TDAn** and **TDAnPh**, respectively. Similar to the geometry optimized structures, the crystal structures of the **TDAn**[16] and **TDAnPh**[16] also exhibited highly twisted non-planar conformations with eminent torsional angles of 60.6° and 71.1°, respectively, between TDP and anthracene moieties. Unfortunately, we were not able to obtain single crystals with good quality for **TDPy** due to its poor solubility in common organic solvents. Nevertheless, with similar structural distortion parameters for **TDAn** and **TDAnPh** obtained from their single crystal analysis and computational results, the calculated structure for **TDPy** could

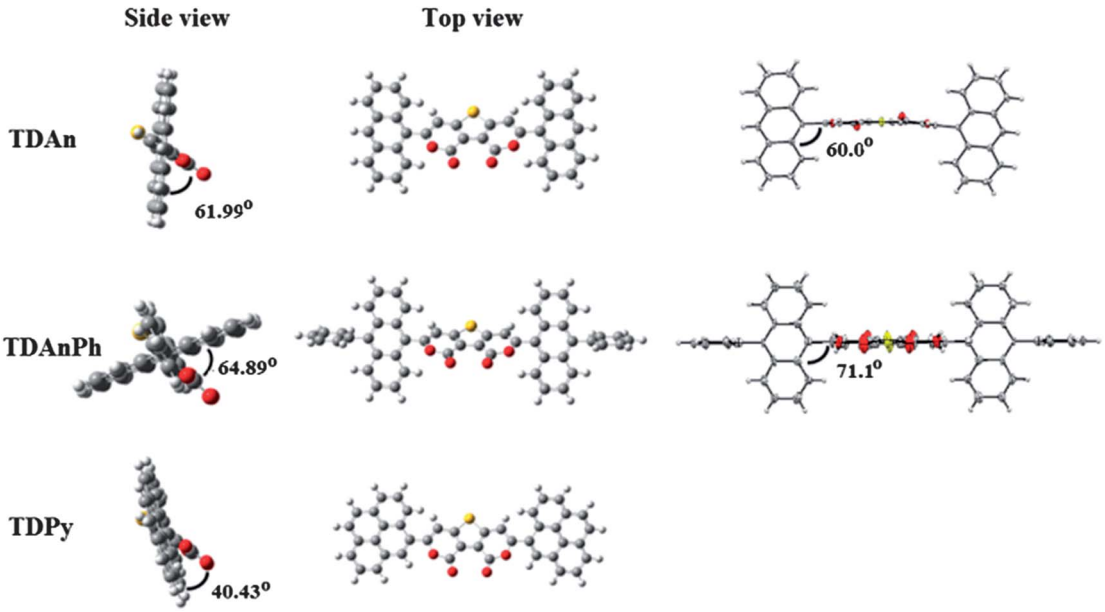

Fig. 3 Calculated optimized conformational structures (left) and crystal structures (right) of **TDAn**, **TDAnPh** and **TDPy**.

provide a good reference to rationalize its solid-state emissive behaviors.

Aggregation induced emission

To further confirm AIE properties of **TDAn** and **TDAnPh**, absorption and photoluminescence in THF–water mixtures were studied in detail. The absorption spectra of **TDAn** and **TDAnPh** exhibited no significant change until the water fraction was increased to 70% where the absorption spectrum was broad with levelling-off of the tail in the visible region due to Mie effect or light scattering because of the formation of nanoscopic aggregates (Fig. 4a and b).[17] The PL spectra of the **TDAn** and **TDAnPh** in the water–THF mixtures with different water contents are illustrated in Fig. 4c and d. The PL intensities of **TDAn** and **TDAnPh** in dilute THF solutions were weak and decreasing in their intensities was observed as the water content increased up to 50%. However, the emission abruptly increased with a concomitant blue shift with a water fraction up to 60–70%. Thus, the increase in PL intensity can be attributed to the AIE effect caused by the formation of molecular aggregates when water is added into the solution. The Φ_f of **TDAn** and **TDAnPh** increases drastically to 13 and 21%, respectively, in THF–water as the nano-aggregates formed. The increased fluorescence quantum yields in the aggregation state with respect to the solution state could be attributed to the restricted intramolecular rotations (RIR). In molecularly dissolved solutions, the intramolecular torsional motion is relatively free which facilitates the non-radiative relaxation pathways and affords weak fluorescence emission. However, in aqueous media, the intramolecular vibration and rotations are restricted due to the formation of aggregates to exhibit the aggregation-induced emission enhancement. The colors of these compounds in THF–water mixtures with different water fractions are significantly different (insets of Fig. 4c and d). This can be attributed to the formation of various aggregation states of the molecules such as crystalline and amorphous particles in the mixed solvent.

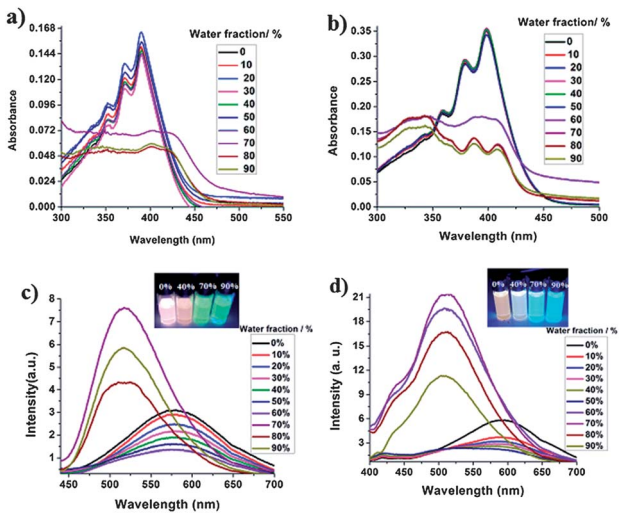

Fig. 4 Absorption and PL spectra of **TDAn** (a and c) and **TDAnPh** (b and d) in various THF–water mixtures. The insets of (c) and (d) show the fluorescence images of **TDAn** and **TDAnPh** with various water fractions (from left to right: 0%, 40%, 70%, and 90%) under UV light (365 nm).

Piezo-fluorochromism

One common structural feature for the class of AIE compounds is that multiple peripheral phenyl groups are linked to an olefinic core with examples including distyrylanthracenes, cyanodistyrylbenzene, silole, triphenylethylene, and tetraphenylethylene derivatives *etc.*[14,18] Due to the large steric hindrance between the phenyl rings the AIE molecules adopt a twisted

conformation which reduces the π–π interactions. In this regard, the weak molecular interaction leads to defects in the crystals and can be readily destroyed by applying an external pressure. The applied pressure induces planarization of the molecular conformation because of the release of the twist stress and, thus, results in a red shift of the emission spectrum. The original conformation can be recovered simply by heating. The phenomena of fluorescent switching by grinding and heating can be termed as piezochromic aggregation induced emission (PAIE).[14,18] Both **TDAn** and **TDAnPh** exhibited prominent PAIE properties. Upon grinding the as-synthesized compounds with a pestle, the green (507 nm) and bluish green (491 nm) emissive solids of **TDAn** and **TDAnPh** changed to yellow emissive solids (Fig. 5a) and showed emission maxima at 548 and 540 nm, respectively, for **TDAn** and **TDAnPh** (Fig. 1a and b) and the quantum yields (Φ_f) of ground **TDAn** and **TDAnPh** samples were found to be 4.1% and 5.3% respectively. Obviously, the appearance of pressure induced emission changes in **TDAn** and **TDAnPh** indicates that these compounds behave as piezochromic materials. The precise matching of ^{1}H NMR and MALDI-TOF mass spectra of the ground samples of **TDAn** and **TDAnPh** to their corresponding as-synthesized samples implies that no chemical reactions occurred during the grinding process and the different luminescence properties are truly ascribed to the physical processes such as change in the intermolecular packing and phase transition. The orange emissive ground solids can be reverted back to the as-synthesized materials upon annealing the ground samples at 140 °C for **TDAn** and 250 °C for **TDAnPh** for about 5 min or recrystallizing from a dichloromethane solution. The reversible switching of the emission wavelengths can be realized by the repeated process of grinding and heating without decomposition of the samples (Fig. 5b and c). The switchable color change feature of the compounds may render them promising candidates for temperature or pressure sensing as well as optical recording materials.

To obtain insights into the phase transition and molecular packing, powder X-ray diffraction (XRD) and differential scanning calorimetry (DSC) experiments were performed. The as-synthesized compounds for both **TDAn** and **TDAnPh** clearly exhibited sharp and intense reflections in their XRD profiles indicative of microcrystalline structures. In contrast, the ground samples did not show any noticeable XRD patterns, which suggests the ground samples are amorphous. Similar XRD signals to those in the as-synthesized samples appeared when the ground samples were heated (Fig. 6a and b). Thus, the transformation of green or blue-green fluorescent to orange emission is imputed to phase transition and is completely reversible under treatment of grinding (or pressing) and annealing (or re-crystallizing from solvent). No peak was observed up to 300 °C in the DSC diagram for as-synthesized samples of both **TDAn** and **TDAnPh**. However, the corresponding ground samples exhibited a clear exothermic peak at 134 and 250 °C for **TDAn** and **TDAnPh**, respectively (Fig. 6c and d). This thermal behavior is ascribed to a solid–solid transformation, *i.e.* the meta-stable state of the ground samples to a more stable state by annealing.[19] On the basis of PXRD, as well as solid and frozen state emission data, it can be rationalized that both **TDAn** and **TDAnPh** possess a highly twisted conformation in the solid state which is stabilized by various secondary bonding interactions. However, the molecular conformation becomes planar to some degree in the amorphous state which leads to close packing and stronger intermolecular interactions. The increased intramolecular conjugation caused by the planarity in amorphous samples might induce red shifts in the PL spectra relative to crystalline samples. On the other hand, these increased intermolecular interactions might propagate a photo-induced electron transfer process which effectively deactivates the emitting state and decreases Φ_f significantly, as evident by the Φ_f of the ground samples.

Acido-fluorochromism

Another interesting phenomenon of the current system is that **TDAn** exhibits selective and pronounced acido-chromic

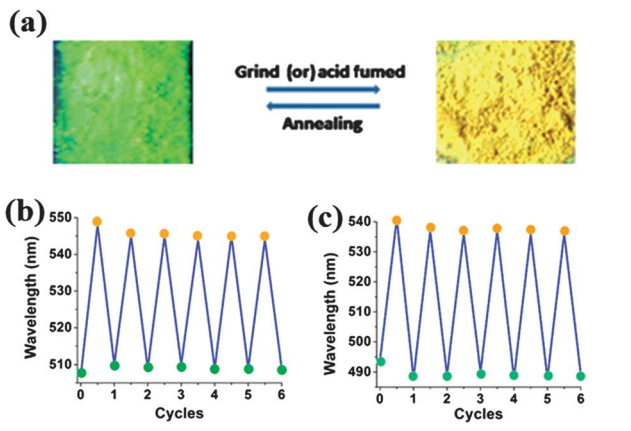

Fig. 5 Photographs of the ground (or acid-fumed) and the annealed samples of **TDAn** under UV light (365 nm) (a); emission wavelengths of the repeated grinding and annealing treatments of **TDAn** (b) and **TDAnPh** (c).

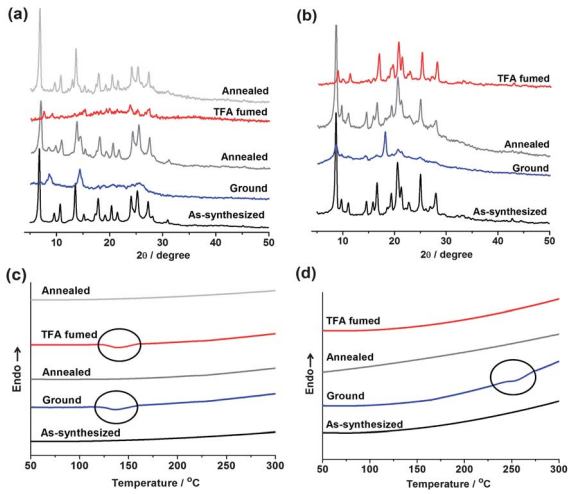

Fig. 6 XRD (top) and DSC (bottom) profiles of **TDAn** (a and c) and **TDAnPh** (b and d).

luminescence. As shown in Fig. 5a, after exposure of the as-synthesized **TDAn** to trifluoroacetic acid (TFA) vapor for 2 min or longer, the bluish green emission changed to yellow emission. The vapor chromic experiments have also been tested with different acids such as $BF_3 \cdot Et_2O$, $POCl_3$, and $SOCl_2$, which showed similar phenomena to TFA (Fig. 7a). The resulting yellow emissive sample appeared virtually the same to the ground sample in both color and the emission maxima (544 nm) and the emission was readily switched back to its original bluish green emission at 507 nm by heating the sample at 140 °C for 5 min. It is worth mentioning that approximately 70% of the **TDAn** sample turned to yellow emissive solid upon acid-exposure while a thin-film displayed complete conversion. Similar to **TDAn** ground sample, the acid-fumed sample (Φ_f = 3.2%) also exhibited a lower quantum yield due to acid induced enhanced intermolecular interactions. The low quantum yield of the acid-fumed solid could also be attributed to a similar mechanistic process occurring in the ground samples. The phase transition from the crystalline powder to amorphous solid can be realized by exposure to the acid vapor. Thermal annealing of the acid-exposed solid reverts to its original crystalline state. It is worth noting that only a 5 nm bathochromic shift in the PL spectrum in a toluene solution of **TDAn** was observed in the presence of acid, indicative of the substantial effect in the solid state due to the phase transition from crystalline to amorphous state. The reversibility of the emission was confirmed by a repeated process of acid exposure and heating treatments (Fig. 7b). In contrast, the acidochromic modulation was not observed for **TDAnPh** even after prolonged exposure to acid vapor. The XRD pattern for acid-fumed **TDAn** showed very weak and broad diffraction signals indicating the structural changes in molecular aggregation from crystalline to amorphous state (Fig. 6a). As expected, acid-fumed **TDAn** showed an exothermic peak at 134 °C in its DSC diagram, which exactly matches the phase transition temperature of **TDAn** ground sample (Fig. 6c). Intense and sharp XRD reflection peaks are also similar to its as-synthesized compound and the absence of DSC phase transition signal suggests no effect of acid on its molecular packing in **TDAnPh** (Fig. 6b and d).

In order to understand the structure–property relationship of specific acido-chromic characteristics of **TDAn** over **TDAnPh**, a comparison of the molecular arrangements in the crystal structures by X-ray structural analysis has been performed. The molecular packing is certainly driven by the intermolecular interactions such as π–π, C–H···π and C–H···X (X = F, O, N, S *etc.*) that can be used to tune the solid-state molecular arrangements and plays a crucial role in the stability of the crystal packing. The crystal structure of **TDAn** adopts a so-called sandwich herringbone type[20] of pattern in which dimers of **TDAn** are arranged in a herringbone manner by the coexistence of two types of interactions (Fig. 8a). A face-to-face π stacking interaction to form dimer (3.56 Å) and two face-to-edge inter-dimer C–H···O (2.87 Å) interactions result in the sandwich herringbone. Two monomeric units in the **TDAn** dimer overlap perfectly in their long molecular axis while an ~80% of convergence was noticed in the short-molecular axis. Moreover, two **TDAn** molecules form an anti-parallel arrangement in the dimer and two solvent DMSO molecules also co-crystallized per unit of the **TDAn** dimer. These two kinds of intermolecular interactions play a substantial role in **TDAn** to form the herringbone arrangement and the molecules with herringbone stacking structure are known to possess minimal π–π stacking interactions.[21] On the other hand, the additional phenyl substituents in **TDAnPh** heavily influenced the crystal packing to form a one-dimensional slipped π-stacking along the molecular long axis. The adjacent anthracene planes overlapped with each other by about 33% and the vertical average intermolecular distance of 3.60 Å suggests prominent π–π interactions between the molecules (Fig. 8b). Besides the strong π–π interactions, there were also eight C–H···π interactions between the anthracene and phenyl substituents with four adjacent molecules along the short molecular axis (Fig. 8c). From the above findings, it can be rationalized that the acid will protonate the carbonyl oxygen upon acid vapor exposure and diminish the relatively weak intermolecular interactions in **TDAn**, whereas the strong synergetic intermolecular π–π and C–H···π interactions in **TDAnPh** override the effect of acid.

Conclusions

In summary, we have demonstrated two new TDP grafted anthracene derivatives exhibiting AIE and piezochromic

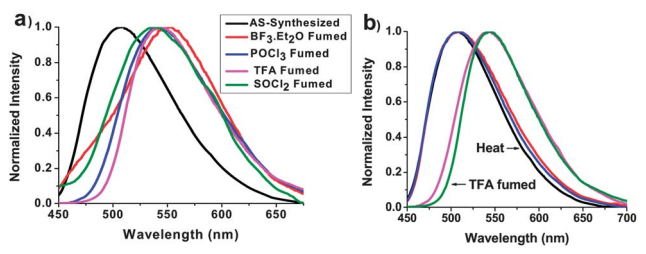

Fig. 7 (a) Overlay of solid-state PL spectra for as-synthesized and various acid-fumed **TDAn**; (b) The PL spectra of **TDAnPh** in repeated conversions between acid fuming and heating treatments.

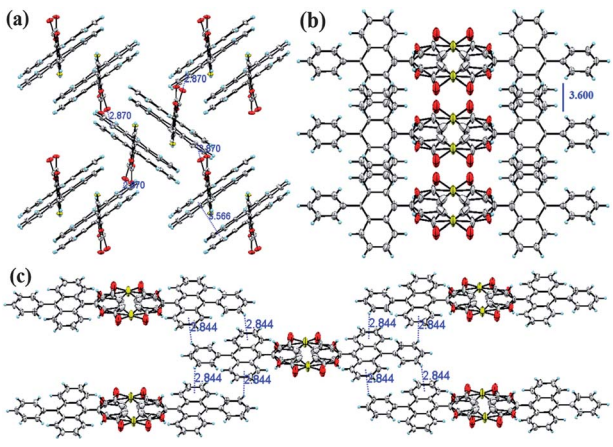

Fig. 8 Crystal packing modes of (a) **TDAn** (b) & (c) **TDAnPh**. The co-crystallized DMSO molecules in **TDAn** were omitted for clarity. The central TDP core showed severe crystallographic disorder in the **TDAnPh** crystal structure.

properties in which emission colors can be switched by grinding and heating. Based on XRD, DSC, and NMR studies, the PL change is attributed to a result of structurally ordered to disordered phase transition. We also found that one of the anthracene derivatives, **TDAn**, displayed specific acido-chromism, whereas the other congener, **TDAnPh**, did not. On the basis of crystal structure analysis, we concluded that the change of crystalline to amorphous state was due to the lack of strong intermolecular interactions. The current study has disclosed a class of new stimuli-responsive materials with great potentials in applications for micro-environmental sensing, optical switching and recording.

Experimental section

All chemical reagents were commercially available and were used without further purification unless otherwise noted. All reactions were monitored using pre-coated TLC plates and purified by column chromatography. Column chromatography was performed on silica (60–120 mesh). ^{1}H NMR and ^{13}C NMR spectra (δ values, ppm) were recorded using Bruker AVANCE III 400 MHz, Ultra Shield 400 and 500 MHz NMR spectrometers. Absorption and fluorescence spectra were obtained with a Varian Cary 300 UV-vis spectrophotometer and Jobin-Yvon FL3-21 Horiba fluorolog fluorimeter, respectively. Fluorescence quantum yields were measured using 9,10-diphenylanthracence (DPA) in cyclohexane as a standard reference. Solid-state emission quantum yields were determined by the Jobin-Yvon FL3-21 Horiba fluorolog fluorimeter equipped with an integrated sphere.[22] Thermal transitions were collected by a Perkin-Elmer Thermal Analysis DSC7 under nitrogen at a heating rate 10 °C min^{-1}. Powder XRD patterns of the samples were recorded on a Philips X'Pert XRD System. Compounds 3,4-dicyanothiophene (**6**),[23] thiophene-3,4-di(ethylcarboxylate) (**5**)[24,25] thiophene-2,6-dibromo-3,4-di(ethylcarboxylate) (**4**)[26] were synthesized by following the literature.

Thiophene-2,6-dibromo-3,4-di(ethylcarboxylate) (4)

Bromine (15.04 g, 95.2 mmol) was added drop-wise to compound **5** (2 g, 23.8 mmol) in chloroform (3 mL). On completion of bromine addition, the temperature of the reaction mixture was raised from room temperature to 60–70 °C and kept for 12 h. The reaction mixture was then poured into aq. sodium hydroxide solution and extracted with dichloromethane. The organic layer was washed with water, saturated $NaHCO_3$ solution and brine. Removal of the solvent yielded compound **4** as a white crystalline solid in 85% yield. ^{1}H NMR (400 MHz, $CDCl_3$): 4.37 (q, J = 14.4, 7.2 Hz, 4H), 1.37 (t, J = 7.6, 6H); ^{13}C NMR (125 MHz, $CDCl_3$): 161.29, 133.79, 115.60, 61.89,14.01.

General procedure for preparation of compounds 1–3

Solutions of compound **4** (1.3 mmol) and the corresponding alkyne (3.0 mmol, 2.2 equiv.) in dry THF–triethylamine (3 : 1) were coupled in the presence of catalytic amounts of $PdCl_2(PPh_3)_2$ (3 mol %) and CuI (2 mol %) at 50 °C for 16 h under a nitrogen atmosphere. After cooling to room temperature, brine (50 mL) was added and the reaction mixture was extracted with CH_2Cl_2 and dried over Na_2SO_4. The solvent was evaporated under reduced pressure and the residue was purified by column chromatography on silica gel to furnish the corresponding products.

Diethyl 2,5-bis(anthracen-9-ylethynyl)thiophene-3,4-dicarboxylate (1)

^{1}H NMR (400 MHz, $CDCl_3$): 8.64 (d, J = 8.8 Hz, 4H), 8.51 (s, 2H), 8.05 (d, J = 8.4 Hz, 4H), 7.66 (t, J = 7.4 Hz, 4H), 7.55 (t, J = 7.4 Hz, 4H), 4.53 (q, J = 14, 7.2 Hz), 1.43 (t, J = 7.0 Hz); ^{13}C NMR (125 MHz, $CDCl_3$): 162.67, 135.17, 132.97, 131.09, 129.22, 128.77, 127.19, 126.51, 125.88, 115.70, 97.06, 91.20, 61.88, 14.20; HRMS (MALDI): m/z calcd for $C_{42}H_{29}O_4S$: 629.1786 $[M + H]^+$; found: 629.1807.

Diethyl 2,5-bis(10-phenylanthracen-9-ylethynyl)thiophene-3,4-dicarboxylate (2)

^{1}H NMR (400 MHz, $CDCl_3$): 8.73 (d, J = 8.8 Hz, 4H), 8.27–8.20 (m, 8H), 7.71–7.57 (m, 14H), 7.45–8.41 (m, 8H), 4.55 (q, J = 14.4, 7.2 Hz, 4H), 1.44 (t, J = 7.2 Hz, 6H); ^{13}C NMR (125 MHz, $CDCl_3$): 162.94, 140.25, 138.44, 135.41, 132.89, 131.20, 130.12, 128.60, 128.00, 127.76, 127.43, 127.12, 126.86, 125.99, 116.05, 97.59, 91.71, 62.13, 14.48; HRMS (MALDI): m/z calcd for $C_{54}H_{36}O_4S$: 780.2333 $[M + H]^+$; found: 780.2350.

Diethyl 2,5-bis(pyren-1-ylethynyl)thiophene-3,4-dicarboxylate (3)

^{1}H NMR (400 MHz, $CDCl_3$): 8.68 (d, J = 5.2 Hz, 2H), 8.27–8.20 (m, 8H), 8.15–8.13 (m, 4H), 8.08–8.04 (m, 4H), 4.54 (q, J = 14.4, 7.2 Hz, 4H), 1.46 (t, J = 7.2 Hz, 6H); ^{13}C NMR (125 MHz, $CDCl_3$): 162.90, 135.45, 132.53, 132.25, 131.36, 131.19, 129.86, 129.04, 128.98, 127.37, 126.68, 126.58, 126.20, 126.11, 125.53, 124.73, 124.57, 124.35, 116.40, 99.28, 86.01, 62.07, 14.48; HRMS (MALDI): m/z calcd for $C_{46}H_{30}O_4S$: 676.1708 $[M]^+$; found: 676.1723.

General procedure for preparation of TDAn, TDAnPh and TDPy

Compounds **1–3** (0.7 mmol) were dissolved in trifluoroacetic acid (10 mL) and the mixtures were refluxed at 70 °C. The progress of the reaction was monitored by TLC. After 24 h, the reaction mixture was poured into water (300 mL) and the filtrate thereby formed was washed with aq. $NaHCO_3$ solution to remove excess of acid. The crude mixture was repeatedly washed with diethyl ether and methanol to yield pure compounds in 61–68% yields.

3,7-Di(anthracen-9-yl)thieno[3,2-*c*:4,5-*c*′]dipyran-1,9-dione (TDAn)

^{1}H NMR (400 MHz, DMSO): 8.90 (s, 2H), 8.26–8.23 (m, 4H), 8.10–8.08 (m, 4H), 7.75 (s, 2H), 7.68–7.62 (m, 8H); ^{13}C NMR (125 MHz, DMSO): 134.68, 132.17, 131.58, 131.50, 130.72, 129.96, 129.53, 128.89, 128.80, 127.60, 126.85, 125.92, 125.05; HRMS

(MALDI): *m*/*z* calcd for $C_{38}H_{21}O_4S$: 573.1160 $[M + H]^+$; found: 573.1180.

3,7-Bis(10-phenylanthracen-9-yl)thieno[3,2-*c*:4,5-*c*′]dipyran-1,9-dione (TDAnPh)

^1H NMR (400 MHz, $CDCl_3$): 8.04 (d, $J = 8.4$ Hz, 4H), 7.73 (d, $J = 8.8$ Hz, 4H), 7.65–7.52 (m, 10H), 7.47–7.39 (m, 8H), 7.15 (s, 2H); ^{13}C NMR (125 MHz, $CDCl_3$): 158.18, 155.53, 150.67, 141.14, 138.43, 131.17, 130.44, 129.98, 128.68, 128.06, 127.71, 127.07, 125.86, 125.63, 125.20, 120.21, 105.14; HRMS (MALDI): *m*/*z* calcd for $C_{50}H_{29}O_4S$: 725.1786 $[M + H]^+$; found: 725.1795.

3,7-Di(pyren-1-yl)thieno[3,2-*c*:4,5-*c*′]dipyran-1,9-dione (TDPy)

^1H NMR (400 MHz, $CDCl_3$): 8.66 (d, $J = 9.2$ Hz, 2H), 8.45–8.15 (m, 14H), 8.17 (t, $J = 7.6$Hz, 2H), 7.89 (s, 2H); ^{13}C NMR spectrum was not acquired due to poor solubility in solvents; HRMS (MALDI): *m*/*z* calcd for $C_{42}H_{25}O_4S$: 621.1160 $[M + H]^+$; found: 676.1175.

Acknowledgements

We are grateful to the National Council of Taiwan (Grant no. 100-2628-M-001-002-MY3) and Academia Sinica for support of this research. R. R. M. thanks the postdoctoral fellowship sponsored by the National Science Council of Taiwan (Grant no. 101-2811-M-001-181). Dr Yu-Sheng Wen at Institute of Chemistry, Academia Sinica and Mr Ting-Shen Kuo at National Taiwan Normal University are acknowledged for their help in crystal structure refinement.

Notes and references

1 (*a*) *Luminescent Materials and Applications*, ed. A. Kitai, John Wiley & Sons, Chichester, 2008; (*b*) Z. M. Hudson and S. Wang, *Acc. Chem. Res.*, 2009, **42**, 1584; (*c*) T. M. Figueira-Duarte and K. Müllen, *Chem. Rev.*, 2011, **111**, 7260; (*d*) F. Gao, Q. Liao, Z.-Z. Xu, Y.-H. Yue, Q. Wang, H.-L. Zhang and H.-B. Fu, *Angew. Chem., Int. Ed.*, 2010, **49**, 732.

2 (*a*) Z. Ning, Z. Chen, Q. Zhang, Y. Yan, S. Qian, Y. Cao and H. Tian, *Adv. Funct. Mater.*, 2007, **17**, 3799; (*b*) S. J. Toal, K. A. Jones, D. Magde and W. C. Trogler, *J. Am. Chem. Soc.*, 2005, **127**, 11661; (*c*) J. R. Kumpfer, J. Jin and S. J. Rowan, *J. Mater. Chem.*, 2010, **20**, 145; (*d*) C. Y. K. Chan, Z. Zhao, J. W. Y. Lam, J. Liu, S. Chen, P. Lu, F. Mahtab, X. Chen, H. H. Y. Sung, H. S. Kwok, Y. Ma, I. D. Williams, K. S. Wong and B. Z. Tang, *Adv. Funct. Mater.*, 2012, **22**, 378.

3 A. Kishimura, T. Yamashita, K. Yamaguchi and T. Aida, *Nat. Mater.*, 2005, **4**, 546.

4 M. Burnworth, L. Tang, J. R. Kumpfer, A. J. Duncan, F. L. Beyer, G. L. Fiore, S. J. Rowan and C. Weder, *Nature*, 2011, **472**, 334.

5 J. R. Kumpfer and S. J. Rowan, *J. Am. Chem. Soc.*, 2011, **133**, 12866.

6 (*a*) S. C. Yu, C. C. Kwok, W. K. Chan and C. M. Chen, *Adv. Mater.*, 2003, **15**, 1643; (*b*) W. Ng, X. Gong and W. K. Chan, *Chem. Mater.*, 1999, **11**, 1165; (*c*) M. Shimizu, R. Kaki, Y. Takeda, T. Hiyama, N. Nagai, H. Yamagishi and H. Furutani, *Angew. Chem., Int. Ed.*, 2012, **51**, 4095.

7 (*a*) R. Davis, N. S. S. Kumar, S. Abraham, C. H. Suresh, N. P. Rath, N. Tamaoki and S. Das, *J. Phys. Chem. C*, 2008, **112**, 2137; (*b*) H. Tong, Y. N. Hong, Y. Q. Dong, Y. Ren, M. Haussler, J. W. Y. Lam, K. S. Wong and B. Z. Tang, *J. Phys. Chem. B*, 2007, **111**, 2000; (*c*) H. Y. Zhang, Z. L. Zhang, K. Q. Ye, J. Y. Zhang and Y. Wang, *Adv. Mater.*, 2006, **18**, 2369; (*d*) Y. Mizobe, N. Tohnai, M. Miyata and Y. Hasegawa, *Chem. Commun.*, 2005, 1839; (*e*) Z. Zhao, Z. Wang, P. Lu, C. Y. K. Chan, D. Liu, J. W. Y. Lam, H. H. Y. Sung, I. D. Williams, Y. Ma and B. Z. Tang, *Angew. Chem., Int. Ed.*, 2009, **48**, 7608; (*f*) Z. Zhang, B. Xu, J. Su, L. Shen, Y. Xie and H. Tian, *Angew. Chem., Int. Ed.*, 2011, **50**, 11654; (*g*) T. Mutai, H. Tomoda, T. Ohkawa, Y. Yabe and K. Araki, *Angew. Chem., Int. Ed.*, 2008, **47**, 9522.

8 (*a*) S. J. Yoon, J. W. Chung, J. Gierschner, K. S. Kim, M. G. Choi, D. Kim and S. Y. Park, *J. Am. Chem. Soc.*, 2010, **132**, 13675; (*b*) J. W. Chung, Y. You, H. S. Huh, B.-K. An, S.-J. Yoon, S. H. Kim, S. W. Lee and S. Y. Park, *J. Am. Chem. Soc.*, 2009, **131**, 8163; (*c*) Y. Sagara, T. Mutai, I. Yoshikawa and K. Araki, *J. Am. Chem. Soc.*, 2007, **129**, 1520; (*d*) G.-G. Shan, H.-B. Li, H.-Z. Sun, D.-X. Zhu, H.-T. Cao and Z.-M. Su, *J. Mater. Chem. C*, 2013, **1**, 1440; (*e*) X. Sun, X. Zhang, X. Li, S. Liu and G. Zhang, *J. Mater. Chem.*, 2012, **22**, 17332; (*f*) Y. Ooyama and Y. Harima, *J. Mater. Chem.*, 2011, **21**, 8372; (*g*) G. Zhang, J. Lu, M. Sabat and C. L. Fraser, *J. Am. Chem. Soc.*, 2010, **132**, 2160; (*h*) G.-G. Shan, H.-B. Li, H.-T. Cao, D.-X. Zhu, P. Li, Z.-M. Su and Y. Liao, *Chem. Commun.*, 2012, **48**, 2000; (*i*) Y. Ren, W. H. Kan, V. Thangadurai and T. Baumgartner, *Angew. Chem., Int. Ed.*, 2012, **51**, 3964; (*j*) D. Yan, J. Lu, J. Ma, S. Qin, M. Wei, D. G. Evans and X. Duan, *Angew. Chem., Int. Ed.*, 2011, **50**, 7037; (*k*) X. Gu, J. Yao, G. Zhang, Y. Yan, C. Zhang, Q. Peng, Q. Liao, Y. Wu, Z. Xu, Y. Zhao, H. Fu and D. Zhang, *Adv. Funct. Mater.*, 2012, **22**, 4862; (*l*) B. Xu, Z. Chi, J. Zhang, X. Zhang, H. Li, X. Li, S. Liu, Y. Zhang and J. Xu, *Chem.–Asian J.*, 2011, **6**, 1470; (*m*) G. R. Krishna, M. S. R. N. Kiran, C. L. Fraser, U. Ramamurty and C. M. Reddy, *Adv. Funct. Mater.*, 2013, **23**, 1422; (*n*) M. Rajeswara Rao, C.-W. Liao, W.-L. Su and S.-S. Sun, *J. Mater. Chem. C*, 2013, **1**, 5491–5501.

9 (*a*) R. Matsushima, N. Nishimura, K. Goto and Y. Kohno, *Bull. Chem. Soc. Jpn.*, 2003, **76**, 1279; (*b*) T. Mutai, H. Satou and K. Araki, *Nat. Mater.*, 2005, **4**, 685; (*c*) E. Takahashi, H. Takaya and T. Naota, *Chem.–Eur. J.*, 2010, **16**, 4793.

10 W. R. Browne, M. M. Pollard, B. de Lange, A. Meetsma and B. L. Feringa, *J. Am. Chem. Soc.*, 2006, **128**, 12412.

11 (*a*) A. A. Rachford and F. N. Castellano, *Inorg. Chem.*, 2009, **48**, 10865; (*b*) X. Wang, J. Lu, W. Shi, F. Li, M. Wei, D. G. Evans and X. Duan, *Langmuir*, 2010, **26**, 1247; (*c*) B. Y. Zhao, H. Gao, Y. Fan, T. Zhou, Z. Su, Y. Liu and Y. Wang, *Adv. Mater.*, 2009, **21**, 3165; (*d*) D. Cauzzi, R. Pattacini, M. Delferro, F. Dini, C. D. Natale, R. Paolesse, S. Bonacchi, M. Montalti, N. Zaccheroni, M. Calvaresi, F. Zerbetto and L. Prodi, *Angew. Chem., Int. Ed.*, 2012, **51**,

9662; (*e*) G. Máhes, H. Nomura, Q. Zhang, T. Nakagawa and C. Adachi, *Angew. Chem., Int. Ed.*, 2012, **51**, 11311; (*f*) S.-J. Yoon, J. H. Kim, K. S. Kim, J. W. Chung, B. Heinrich, F. Mathevet, P. Kim, B. Donnio, A.-J. Attias, D. Kim and S. Y. Park, *Adv. Funct. Mater.*, 2012, **22**, 61.

12 (*a*) C. Dou, L. Han, S. Zhao, H. Zhang and Y. Wang, *J. Phys. Chem. Lett.*, 2011, **2**, 666; (*b*) J. Tolosa, K. M. Solntsev, L. M. Tolbert and U. H. F. Bunz, *J. Org. Chem.*, 2010, **75**, 523.

13 (*a*) T. Suzuki, S. Shinkai and K. Sada, *Adv. Mater.*, 2006, **18**, 1043; (*b*) C. Dou, D. Chen, J. Iqbal, Y. Yuan, H. Zhang and Y. Wang, *Langmuir*, 2011, **27**, 6323; (*c*) J. W. Chung, B.-K. An and S. Y. Park, *Chem. Mater.*, 2008, **20**, 6750.

14 (*a*) H. Li, X. Zhang, Z. Chi, B. Xu, W. Zhou, S. Liu, Y. Zhang and J. Xu, *Org. Lett.*, 2011, **13**, 556; (*b*) X. Zhang, Z. Chi, J. Zhang, H. Li, B. Xu, X. Li, S. Liu, Y. Zhang and J. Xu, *J. Phys. Chem. B*, 2011, **115**, 7606; (*c*) X. Zhang, Z. Chi, X. Zhou, S. Liu, Y. Zhang and J. Xu, *J. Phys. Chem. C*, 2012, **116**, 23629; (*d*) Y. Dong, B. Xu, J. Zhang, X. Tan, L. Wang, J. Chen, H. Lv, S. Wen, B. Li, L. Ye, B. Zou and W. Tian, *Angew. Chem., Int. Ed.*, 2012, **51**, 10782; (*e*) X. Zhang, Z. Chi, H. Li, B. Xu, X. Li, W. Zhou, S. Liu, Y. Zhang and J. Xu, *Chem.–Asian J.*, 2011, **6**, 808.

15 T. L. Stottand and M. O. Wolf, *J. Phys. Chem. B*, 2004, **108**, 18815.

16 Please see the ESI.†

17 B. Xu, J. He, Y. Dong, F. Chen, W. Yu and W. Tian, *Chem. Commun.*, 2011, **47**, 6602.

18 (*a*) S.-J. Yoon and S. Y. Park, *J. Mater. Chem.*, 2011, **21**, 8338; (*b*) M. S. Kwon, J. Gierschner, S.-J. Yoon and S. Y. Park, *Adv. Mater.*, 2012, **24**, 5487; (*c*) Y. Q. Dong, J. W. Y. Lam, A. J. Qin, Z. Li, J. Z. Sun, Y. P. Dong and B. Z. Tang, *J. Inorg. Organomet. Polym. Mater.*, 2007, **17**, 673; (*d*) X. Zhang, Z. Chi, B. Xu, C. Chen, X. Zhou, Y. Zhang, S. Liua and J. Xu, *J. Mater. Chem.*, 2012, **22**, 18505; (*e*) B. Xu, M. Xie, J. He, B. Xu, Z. Chi, W. Tian, L. Jiang, F. Zhao, S. Liu, Y. Zhang, Z. Xud and J. Xua, *Chem. Commun.*, 2013, **49**, 273; (*f*) J. T. He, B. Xu, F. P. Chen, H. J. Xia, K. P. Li, L. Ye and W. J. Tian, *J. Phys. Chem. C*, 2009, **113**, 9892; (*g*) Y. Hong, J. W. Y. Lam and B. Z. Tang, *Chem. Soc. Rev.*, 2011, **40**, 5361.

19 (*a*) C. Shi, Z. Guo, Y. Yan, S. Zhu, Y. Xie, Y. S. Zhao, W. Zhu and H. Tian, *ACS Appl. Mater. Interfaces*, 2013, **5**, 192; (*b*) Z. Zhang, D. Yao, T. Zhou, H. Zhang and Y. Wang, *Chem. Commun.*, 2011, **47**, 7782.

20 T. Yamamoto, S. Shinamura, E. Miyazaki and K. Takimiya, *Bull. Chem. Soc. Jpn.*, 2010, **83**, 120.

21 (*a*) F. Chen, J. Zhang and X. Wan, *Chem.–Eur. J.*, 2012, **18**, 4558; (*b*) M. Mas-Torrent and C. Rovira, *Chem. Rev.*, 2011, **111**, 4833.

22 Y.-T. Shen, C.-H. Li, K.-C. Chang, S.-Y. Chin, H.-A. Lin, Y.-M. Liu, C.-Y. Hung, H.-F. Hsu and S.-S. Sun, *Langmuir*, 2009, **25**, 8714.

23 Q. T. Zhang and J. M. Tour, *J. Am. Chem. Soc.*, 1997, **119**, 9624.

24 D. W. H. MacDowell and J. C. Wisowaty, *J. Org. Chem.*, 1972, **37**, 1712.

25 E. C. Kornfeld and R. G. Jones, *J. Org. Chem.*, 1954, **19**, 1671.

26 N. Atılgan, F. Algi, A. M. Önal and A. Cihaner, *Tetrahedron*, 2009, **65**, 5776.

